# Isotropic stress reduces cell proliferation in tumor spheroids

# Isotropic stress reduces cell proliferation in tumor spheroids

**Fabien Montel**[1,2,6], **Morgan Delarue**[1,2,5,6], **Jens Elgeti**[1,2],
**Danijela Vignjevic**[1,3], **Giovanni Cappello**[1,2,7]
**and Jacques Prost**[1,2,4]

[1] Institut Curie, Centre de Recherche, Paris F-75248, France
[2] UMR 168, CNRS/Univ Pierre et Marie Curie, Paris F-75248, France
[3] UMR 144, CNRS/Univ Pierre et Marie Curie, Paris F-75248, France
[4] ESPCI, 10 rue Vauquelin, 75005 Paris, France
[5] Univ Paris Diderot, Sorbonne Paris Cité, France
E-mail: giovanni.cappello@curie.fr

**Abstract.** In most instances, tumors have to push their surroundings in order to grow. Thus, during their development, tumors must be able to both exert and sustain mechanical stresses. Using a novel experimental procedure, we study quantitatively the effect of an applied mechanical stress on the long-term growth of a spherical cell aggregate. Our results indicate the possibility to modulate tumor growth depending on the applied pressure. Moreover, we demonstrate quantitatively that the cells located in the core of the spheroid display a different response to stress than those in the periphery. We compare the results to a simple numerical model developed for describing the role of mechanics in cancer progression.

S Online supplementary data available from stacks.iop.org/NJP/14/055008/mmedia

[6] These authors have contributed equally to this work.

[7] Authors to whom any correspondence should be addressed.

**IOP** Institute of Physics · DEUTSCHE PHYSIKALISCHE GESELLSCHAFT

**Contents**

## 1. Introduction

In most instances, tumor growth requires that cells physically push their surroundings to create space to divide. This is a physical force that the cells exert on their microenvironment. The idea that mechanical stresses might play an important role in tissue growth, in developmental biology or in tumor progression, is being increasingly supported (see [1–3] for reviews) by qualitative observations [4–6]. However, a detailed quantitative analysis pinning down numbers is difficult because large tumors are polyclonal, their shapes are often poorly defined, they are heterogeneous and biochemical signaling interferes with mechanics [7, 8]. However, a quantitative knowledge of the mechanical properties of tissues is of paramount importance for understanding tissue growth and tissue invasion.

Thus it is fruitful to start with *in vitro* experiments, where biochemistry and genetics are much easier to control. In particular, one can investigate the properties of tissues using well-defined cell lines and culture media. In this context, cellular aggregates (spheroids) are considered to be good model systems for tissues. In order to study the coupling between tissue growth and mechanical stresses, several groups have been seeding gels with cell aggregates [9–12]: during growth, the cell aggregate has to distort the gel resulting in an elastic stress. The stiffer the gel, the smaller the growth rate of the aggregate and its final size at steady state. These beautiful pioneering experiments allow for a qualitative description of the influence of mechanical stresses on tissue growth and provide the orders of magnitude of the stresses involved [13]. However, they seem to have several limitations. The stress is not constant, but increases during the growth of the cell aggregate. The deformation of the gel due to the aggregate growth becomes larger and nonlinear elastic effects are expected. This is confirmed by the observation of cracks forming in the gel [11]. For all these reasons a precise measurement of the stress opposing the growth seems difficult. Experiments in other geometries that could be

compared to the gel experiments and that would give precise values of the stress are thus highly needed.

From a theoretical point of view, the problem of tissue growth and its interaction with mechanics has been studied using continuum mechanics and computer simulations. Continuum mechanics is appropriate for describing tissues over length scales larger than the cell size and implicitly coarse grains all the phenomena related to the single cell behavior [3, 14–16]. Within this framework, the interaction between a cell and its neighbors is associated with the notion of stress. It has been proposed that this mechanical stress is a key regulator of growth [14, 17–20]. The concept is that at the stationary state/homeostasis the tissue exerts a well-defined pressure, the *homeostatic pressure*, onto its surroundings. If the cell–cell pressure in the tissue is larger than this homeostatic pressure, the tissue shrinks exponentially till it vanishes. On the other hand, for a homogenous tissue, if the pressure is below the homeostatic pressure it grows exponentially. Already by themselves, these simple assumptions lead to novel behaviors such as a nucleation threshold, zero long-term compressibility, competition and fingering instabilities [14, 21]. In computer simulations, the concept of pressure has been implemented as either a 'pressure checkpoint' [22, 23] or a finite 'growth force' [21, 24].

In this paper, we study experimentally the effect of pressure on growth and compare the results closely with continuum theory and simulations. We describe a series of experiments in which the stress is maintained constant at a known value on a spherical cell aggregate over time scales longer than the typical time scales of cell division or apoptosis. This allows measurement of the effect of stress on the aggregate growth. With the use of appropriate biological markers, we also study which of the division or apoptosis rates are most sensitive to stress. In order to interpret our experimental results, we further develop computer simulations that reproduce the experimental observations with a minimum number of hypotheses. These help us to identify the relevant macroscopic parameters and raise new questions. This work follows the short account published previously on this topic [25] and gives additional experimental and numerical evidence.

## 2. Materials and methods

### 2.1. Cell culture and spheroids formation

We prepare colon carcinoma cell spheroids derived from mouse CT26 cell lines (ATCC CRL-2638) using a classical agarose cushion protocol [26]. The wells of a 48-well plate are covered with agarose gel (Ultrapure agarose, Invitrogen, Carlsbad, CA) and cell suspensions are seeded on the gels at a concentration of 20 000 cells per well. Cells self-assemble into spheroids in 24 h. Cells are cultured under 95% air/5% $CO_2$ atmosphere in Dulbecco's modified Eagle's medium (DMEM) enriched with 10% calf serum and antibiotic–antimycotic (culture medium). Using confocal microscopy, we check that the shape of the spheroid is indeed close to a sphere.

### 2.2. Dextran preparation and characterization

The Dextran solutions have been prepared by adding the purified product ($M_w = 100$ kDa, Sigma-Aldrich, St Louis, MO) to cell culture medium. In order to obtain a full solubilization, the dilutions were placed for 1 h at 37 °C. This polymer is known to be neutral and is not metabolized by mammalians cells. We also confirmed that it is neither a growth or a death

factor by plating cells for three days with Dextran and measuring the cell concentration and viability. Pressure calibration has been carried out using a membrane osmometer and dynamic light scattering [27, 28].

### 2.3. Cryosections, immunofluorescence staining and image analysis

Spheroids are embedded in a tissue freezing medium and then frozen at $-80\,°C$ for at least 1 h. Thin slices of $5\,\mu m$ are cut from the spheroid and stored at $-20\,°C$. They are stained using a classical immunofluorescence staining protocol. Slices are fixed using 3.7% PFA/PBS (v/v) and then blocked with a 2% BSA/PBS (w/v) solution at room temperature. Slices are incubated first with anti-Ki67 antibody (Ref AbC10-K006—ABCys Biologie, Paris) or anti-cleaved PARP antibody (Ref 9541—Cell Signaling, Danvers, MA) for an hour and then with fluorescent secondaries and DAPI for nucleus staining for another hour. Images are recorded with an Eclipse Ti Microscope (Nikon Instruments). Using home-made software, we analyze the cryosections. The positions of each nucleus positive for the staining are detected by thresholding the minima of the second derivative of the image. The position of the centroid of the spheroid is calculated by averaging the different positions of the nuclei in the section, and the distances of each nucleus towards the center are calculated. We then plot the distribution of these distances using a sliding box method as described in [29] with a box width of $30\,\mu m$.

### 2.4. Epidermal growth factor diffusion

Spheroids under 0 and 1000 Pa of stress are incubated with Alexa-555-conjugated epidermal growth factor (A555-EGF) at a physiologically relevant concentration ($200\,\mu g\,ml^{-1}$) for 2 days. They are embedded and cut as described in section 2.3, and incubated in 3.7% PFA/PBS (w/w) supplemented with DAPI. Images are then recorded.

### 2.5. Dissipative particle dynamics simulations

In order to simulate the growing spheroids under external pressure as closely to the experimental situation as possible, we adapted existing simulations from [21, 24]. The growing spheroid is surrounded by a number $N_p$ of passive particles that exert a pressure on it. This is similar to the polymer pressing on the tissue spheroid. For simplicity the particles use the same interaction potentials as the cellular particles, but with different parameters. In essence they are single particles, and thus do not grow. They do not adhere ($f$ (particle–particle) $= f$ (particle–cell) $= 0$) and are smaller (by reducing the repulsive force between passive particles $f$ (particle–particle) $\approx$ $0.04\,f$ (cell–cell)). Constant pressure is achieved via the boundary conditions. While we employ periodic boundary conditions in the $x$ and $y$ directions, the $z = 0$ plane is a bounce-back (i.e. no slip, solid) wall. The second $z$ boundary is a movable piston at $z = z_0$. All particles experience a force $f_z \propto -(z - z_0)^{-8}$ due to the piston. The results of simulations are not sensitive to the value of the exponent if this one is large enough. The piston, on the other hand, slowly adapts its position $z_0$ according to the reaction forces and the imposed pressure. The bounce-back wall at $z = 0$ allows an easy control that the pressure in the 'particle gas' is indeed equal to the imposed pressure.

Details of the simulation method can be found in [21]. We use the same parameters as the 'standard tissue' defined therein, except that, for increased adhesion, $f$ (cell–cell) $=$ $1.5 \times f$ (standard) and noise intensity is increased tenfold.
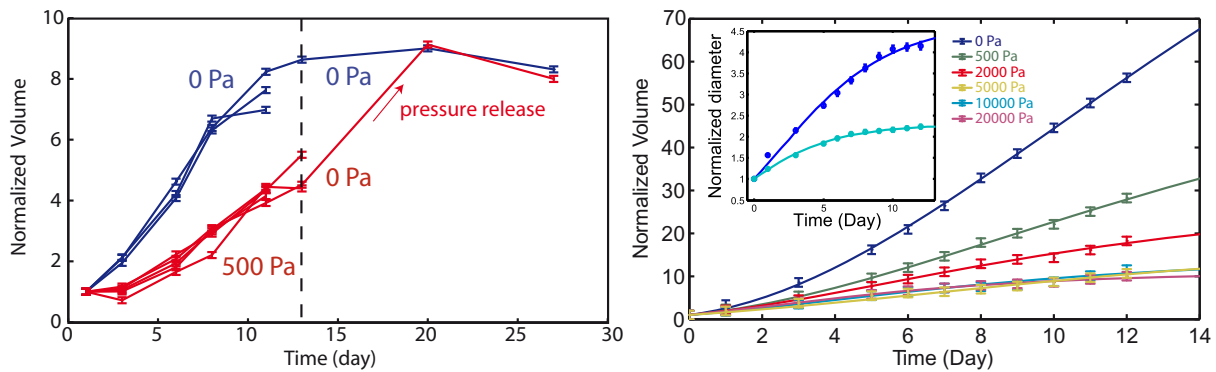
**Figure 1.** Growth curves of individual spheroids under stress. (Left) Normalized volume $V(t)/V(0)$ of individual spheroids as a function of time for the *indirect experiments*. The initial diameter is typically $D_0 = 400\,\mu$m. At $t = 13$ days, stress is released. (Right) Normalized volume of individual spheroids as a function of time for the *direct experiments*. The initial diameter is typically $D_0 = 200\,\mu$m. Points are representative experimental data for individual spheroids taken out of a larger set of experiments. In the inset, we show the normalized diameter of individual spheroids as a function of time for $P = 0\,$Pa and $P = 10\,$kPa. For each condition, $N \geqslant 3$ experiments have been recorded. Points are experimental data and lines are the results of fits with the two-rate model. Error bars are the image analysis errors.

One problem in computer simulations is always the relation to real units. Our experimental results, which we describe in section 3.5, strongly suggest that the bulk division rate $k_{\rm d}$ decays in the 10 kPa range. Conversely, in the simulations this rate decays exponentially, $k_{\rm d} \propto {\rm e}^{-P/P_0}$. We choose units in such a way that the characteristic decay pressure $P_0 = 10\,$kPa.

## 3. Results

### 3.1. Indirect stress measurements

We first carry out *indirect stress measurements*. A growing spheroid is positioned inside a closed dialysis bag (diameter 10 mm, Sigma-Aldrich), which is then placed in an external medium with added Dextran. The dialysis membrane was chosen so that its molecular weight cut-off (10 kDa) prevents the diffusion of Dextran through its pores. Equilibration of the water chemical potential results in an osmotic stress and a force acting on the dialysis membrane. This force is transmitted in quasi-static equilibrium to the spheroid and is calibrated as in [27, 28]. The stress exerted on the cellular system can be seen as a network stress that tends to reduce the volume occupied by the spheroid. It acts directly at the cell level and not on the interstitial fluid. Time lapse images of the spheroids are recorded every 24 h using differential interference contrast microscopy (Axiovert 100, Carl Zeiss). Those images are automatically analyzed to determine the evolution of the spheroid diameter $D(t)$ and volume $V(t)$ (figure 1, left). In the absence of any applied stress, the spheroid reaches a steady state with a typical diameter of $900\,\mu$m corresponding to the balance between the apoptotic core and the proliferating rim as discussed in previous studies [30, 31]. When Dextran is added to the medium, both the growth rate $\frac{{\rm d}V}{{\rm d}t}$ and
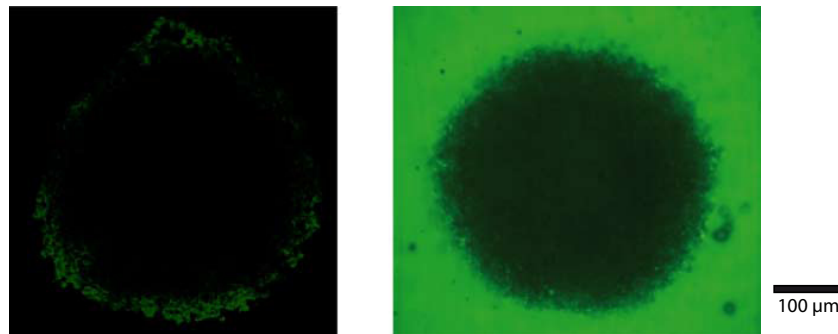
**Figure 2.** Diffusion of Dextran inside the spheroid. (Left) Cryosections and epifluorescence of the same FITC–Dextran. (Right) Confocal imaging of a spheroid in a solution of FITC–Dextran.

the steady-state volume decrease (figure 1, left). Interestingly, after a stress release, the growth of the spheroid resumes until it reaches the same steady-state volume observed in the absence of external pressure. This indicates that the effect of stress is reversible on the time scale of a few days. Altogether, these results show that an external applied stress modulates the growth of tumor spheroids.

### 3.2. Direct stress measurements

We also perform *direct experiments* where the osmotic stress is applied onto the spheroid in the absence of the dialysis membrane. In order to verify that Dextran cannot diffuse inside the spheroid, we place it in a medium supplemented with fluorescent FITC–Dextran at an osmotic stress $\Pi = 1000$ Pa. After 4 days of incubation, the first $70\,\mu$m of the spheroid is imaged using spinning disc microscopy (see figure 2). Moreover, we prepare cryosections to measure Dextran concentration in the bulk of the spheroid. With both techniques we observe that the amount of Dextran able to penetrate the spheroid is negligible compared to the Dextran concentration in the medium (two orders of magnitude decrease in concentration). The osmotic stress is thus applied on the first layer of cells that plays the role of the dialysis membrane in the *direct* experiment and transmits the stress to the rest of the spheroid. The volume of the spheroid has also been measured as a function of time (figure 1, right). The fact that we observe a dependence of the growth rate and the steady-state size on stress very similar to that observed in the *indirect* experiment validates our approach. Interestingly, the steady-state size becomes almost independent of pressure for a stress larger than 10 kPa. We will see in section 3.5 how this observation can be rationalized.

The *direct* experiment is based on the application of a mechanical stress on the surface of the spheroid through an osmotic pressure difference. Osmotic stress is known to have direct effects on cell growth and apoptosis, in particular through the mitogen-activated protein kinase pathway [32–35]. However, in all these studies, such effects are only measured for stresses two orders of magnitude larger than the one applied in our experiments (1 MPa compared to 10 kPa). Moreover, they correspond mainly to instantaneous apoptosis at the surface of the studied tissues through an increased cleavage of PARP and caspase 3. Here, contrary to what was seen in these earlier experiments, we do not observe any apoptosis at the surface of the spheroid where the
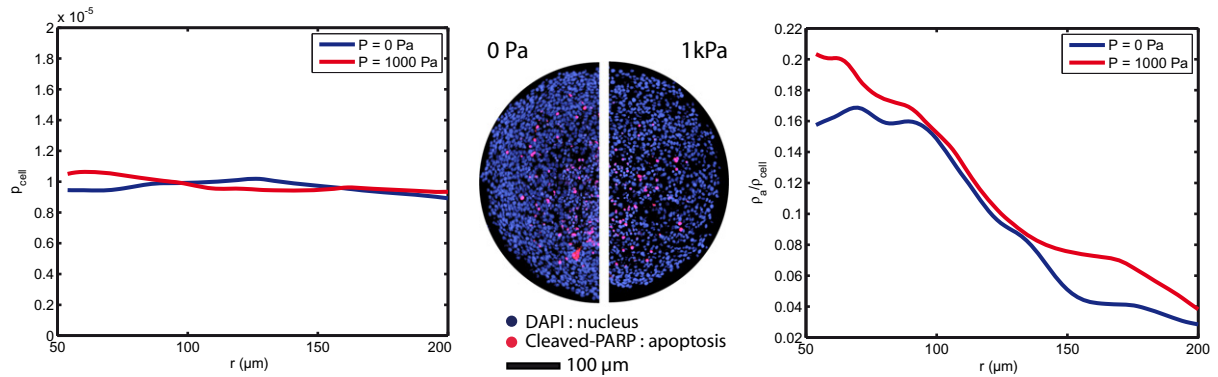
**Figure 3.** Effect of stress on the distribution of cells and apoptosis. (Middle) Cryosections and immunofluorescence staining of the spheroids are used to label the cell nucleus (DAPI in dark blue) and apoptosis (antibody against Cleaved-PARP in red). (Left) Quantification of the cell nucleus radial probability $p_{cell}$. (Right) Quantification of the cell apoptosis relative density $\rho_a/\rho_{cell}$. The spheroid diameters are $400\,\mu$m.

osmotic stress is exerted (figure 3). This shows that we are considering a completely different regime. In addition, one could also wonder if our observations are really resulting from the effect of mechanical stresses or more simply from the change in the concentration of growth factors or salts inside the spheroid as a result of the Dextran concentration outside. It can be checked by balancing chemical potentials that the presence of Dextran outside the spheroid creates a negligible concentration gradient of all other soluble molecules. The concentration difference of a small solute between the interior and the exterior of the spheroid due to the presence of Dextran outside can be estimated as $\Delta c_1/c_1 < 10^{-3}$. The relative variation of concentrations is then small and cannot account for our observations. This estimate and the agreement with experiments performed with the dialysis bag confirm that we are really observing the long-time effects of mechanical stresses. The reason for the negligibly small perturbation of small solute concentrations is that the chemical potential of water in cells is dominated by small ions (mM) and is only slightly modified by the presence of Dextran ($\mu$M). A detailed calculation is presented in the supplementary material, available from stacks.iop.org/NJP/14/055008/mmedia.

### 3.3. Cryosections and immunofluorescence

Finally, we investigate the spatial dependence of cell division and apoptosis using cryosections and immunofluorescence staining (figures 3 and 4). From the cryosections, we derive the cell radial probability density $p_{cell}(r)$, the cell apoptosis relative density $\rho_a/\rho_{cell}(r)$ and the cell division relative density $\rho_d/\rho_{cell}(r)$, which are robust quantifications, independent of the thickness of the slices. We observe that the cell radial probability density $p_{cell}(r)$ is not influenced by stress. Moreover, as in previous studies [26, 36], we observe the accumulation of apoptotic cells at the center of the spheroid (figure 3). Importantly, the apoptosis relative density is weakly affected by stress (10% change in mean value on the cell apoptosis relative density). Regarding the proliferation, in the absence of external stress, cell division is distributed
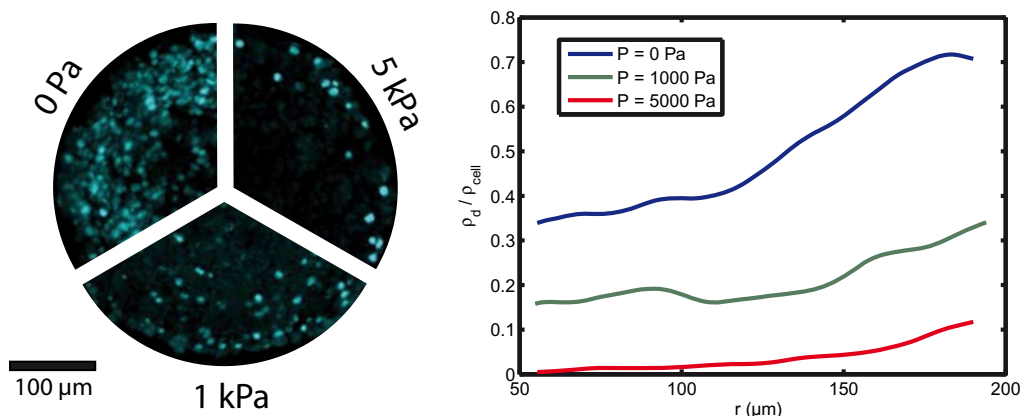
**Figure 4.** Effect of stress on the distribution of proliferation. Cryosections and immunofluorescence staining of the spheroids are used to label the cell divisions (antibody against Ki67 in cyan). (Left) Third sections of a spheroid grown for 2 days in normal medium, with a stress of 1 kPa or with a stress of 5 kPa. (Right) Quantification of the cell division relative density $\rho_d/\rho_{cell}$. The spheroid diameters are 360 $\mu$m.

over all the spheroid with a twofold increase at the periphery (figure 4). For an external stress of 1 kPa or greater, the cell division relative density is largely reduced in the center of the sections. More precisely, the cell division relative density as a function of the radius can be readily fitted by an exponential decay. As detailed in the supplementary material (available from stacks.iop.org/NJP/14/055008/mmedia) we observe that the characteristic decay length of the proliferation $\lambda$ is decreasing weakly (less than 40%) with increasing stress, whereas the division density in the bulk is reduced as by much as a factor of 300 for a 5 kPa stress. To sum up our observations, stress has no effect on the cell distribution in the spheroid, a weak effect on the apoptosis distribution and a strong effect on cell proliferation.

### 3.4. Dissipative particle dynamics simulations

In order to better understand this stress dependence of cell division and to interpret the generic trends of the experimental findings, we have performed numerical simulations similar to those of [21, 24]. We adapt these simulations to the geometry and setup of the experiments. In brief, in the simulations, a cell is represented by a pair of particles which repel each other and thus move apart. When a critical distance is reached, the cell divides. After division, each original particle constitutes, together with a newly inserted particle in its surrounding, a daughter cell. Particles belonging to different cells interact with all particles with a short-range interaction: a constant attractive force describes cell–cell adhesion, while a repulsive short-range potential ensures volume exclusion. The viscous drag between cells is taken into account by a 'Dissipative Particle Dynamics'-type thermostat. Finally, a constant apoptosis rate provides for cell removal. In order to mimic the experiments, tissue spheroids are grown in a container together with a 'passive liquid' under stress. This liquid interacts with the cell particles in a similar way as cell particles with each other and transmits the stress to the spheroid.

As in the experiments, we observe a steady state that depends on the applied stress. In the numerical simulations each division event is easily traced and the spatial distribution
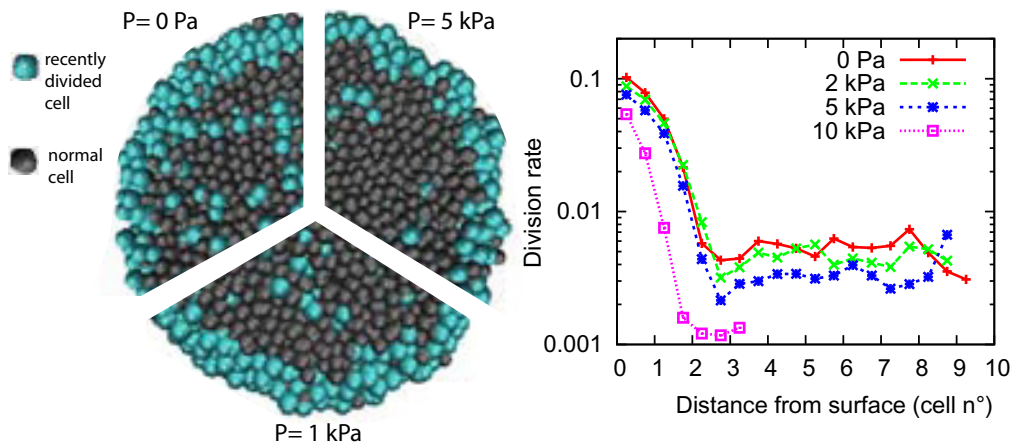
**Figure 5.** Dissipative particle dynamics simulations. (Left) Virtual cryosections of the simulated spheroids for an external pressure $P = 0\,\mathrm{Pa}$, $P = 1\,\mathrm{kPa}$ or $P = 5\,\mathrm{kPa}$. (Right) Quantification of the division rate $k_\mathrm{d}$ as a function of the distance from the surface of the numerical aggregate.



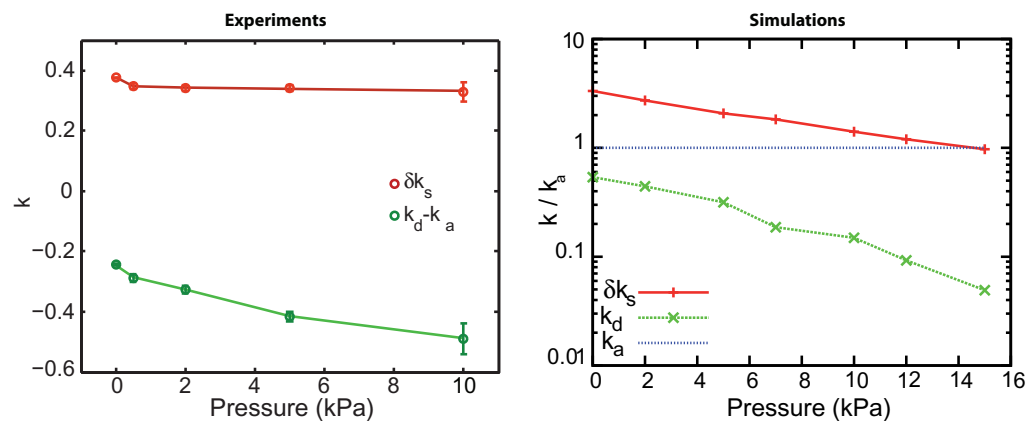**Figure 6.** Evolution of growth rates with stress. (Left) Surface division increment $\delta k_\mathrm{s}$ and bulk growth rate $k = k_\mathrm{d} - k_\mathrm{a}$ as a function of stress. For each condition, $N \geqslant 3$ experiments have been recorded. The error bar are obtained using a jackknifing method and represent the efficiency of the fitting algorithm. (Right) Bulk division rate $k_\mathrm{d}$, surface rate increment $\delta k_\mathrm{s}$ and apoptosis rates $k_\mathrm{a}$ as function of the applied pressure $P$ as extracted from simulations.

of divisions can be measured directly. Furthermore, we construct virtual cryosections of the simulated spheroids for a visual comparison (see figure 5). We observe that the division rate is significantly larger at the surface of the spheroid than in the core, showing a more than tenfold decrease over a few cells distance from the surface. Furthermore, increasing pressure induces a clear decrease of cell division everywhere in the spheroid, but the relative effect is much stronger in the core than at the surface (see also figure 6).

**IOP** Institute of Physics $\Phi$ DEUTSCHE PHYSIKALISCHE GESELLSCHAFT

### 3.5. Two-rate model

Based on the growth curves and cryosection observations, we present an empirical two-rate description of the spheroid growth in the absence or the presence of external stress: the core of the spheroid is mostly undergoing apoptosis whereas its periphery is proliferating [37]. In this situation, the net growth rate is proportional to the area ($\propto r^2$), while the net death rate is proportional to the volume ($\propto r^3$). This surface growth effect leads to a stable steady-state size.

Our two-rate model can be seen as a simplified version of the two-rate model of Radszuweit *et al* [38]. The net bulk growth rate is $k = k_d - k_a$, where $k_d$ and $k_a$ are the division and apoptosis rates, respectively. It is a function of stress. At the surface, the net growth rate $k_d - k_a + \delta k_s$ is larger and $\delta k_s$ has a different stress dependence. Taking into account the surface and bulk growth, the growth equation reads

$$\partial_t N = (k_d - k_a)N + \delta k_s N_s. \tag{1}$$

Assuming a constant cell density and a constant thickness $\lambda$ of the region where the division rate increment is equal to $\delta k_s$, one can (for $R > \lambda$) write a simplified equation for the rate of volume increase:

$$\partial_t V = (k_d - k_a)V + (36\pi)^{1/3}\delta k_s \lambda V^{2/3}. \tag{2}$$

A more detailed calculation is presented in the supplementary material (available from stacks.iop.org/NJP/14/055008/mmedia).

For small spheroids ($R \ll \lambda$) the growth rate ($k_d + \delta k_s - k_a$) is positive and constant, leading to the previously described exponential growth [22, 23]. In our case the growth curves can readily be fitted by equation (2) in the case of large spheroids [39]. The variation with pressure of the parameters $k = k_d - k_a$ and $\delta k_s$ is given in figure 6 (left). The surface rate increment $\delta k_s$ is less affected by stress than the bulk growth rate $k$. A similar fit can be performed on the simulations. The bulk and surface growth rates $k$ and $\delta k_s$ are represented on figure 6 (right). Although both the surface and bulk growth rates depend essentially exponentially on pressure, the decay constant $P_0^s$ of the surface rate is much larger than that of the bulk rate $P_0$. While the bulk rate decreases by more than one order of magnitude, the surface rate decreases by a factor of 3 only. This supports the hypotheses of the simulations. In the experiments, the steady-state size becomes almost independent of pressure for values larger than 10 kPa. This can be explained by the fact that with a negligible bulk division rate, apoptosis rate and surface division rate essentially independent of pressure, the steady-state size would be stress independent. In summary, in both our simulations and experiments, the external stress leads to a strong reduction of cell division in the core, whereas the cell division rate increment at the surface only weakly depends on the external stress.

### 3.6. Proliferative rim, a mechanical explanation

The existence of a proliferative rim in our simulations suggests a purely mechanical contribution towards this effect. Duplication of cells requires a doubling of the occupied volume, which cannot be achieved without working against the stress from the surroundings. In an elastic description of the tissue and its surroundings, this stress is proportional to the elastic modulus. If the cell is located at the surface of the spheroid, most of the deformation field is inside the surrounding material. Thus, any time the surrounding is softer than the tissue, the surface duplication will be faster than in the bulk. A viscous description follows similar arguments
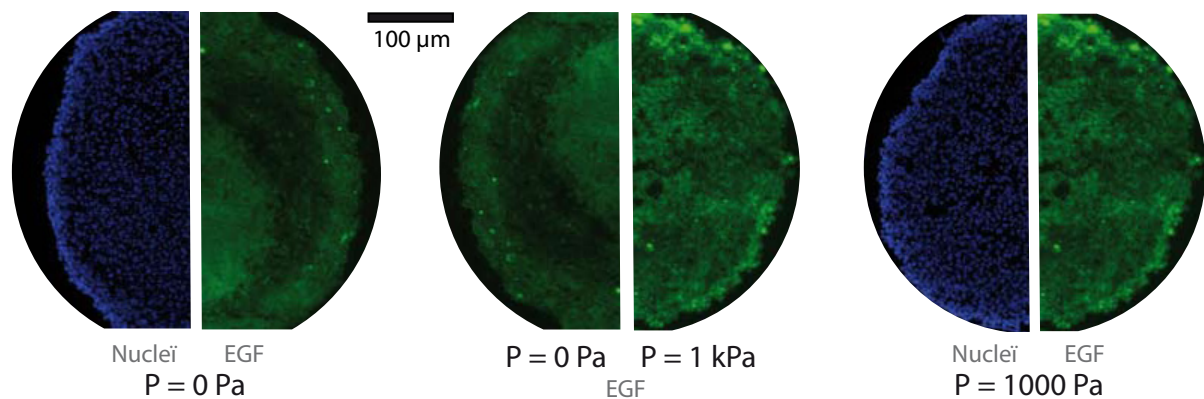
**Figure 7.** Penetration of the EGF growth factor inside a spheroid. Spheroids are incubated with A555-EGF during two days. For $P = 0$ Pa (left) and for $P = 1$ kPa (right) we observe that the growth factor has penetrated in all the spheroid.

and yields similar results. Simulation results show that this mechanical effect could be strong enough to explain the existence of a proliferative rim.

This increased number of cell divisions at the surface drives a cell flow from the surface of the spheroid towards its center. The flow is a possible explanation for the accumulation of apoptotic markers in the center of the spheroid [40].

Another possible contribution to the existence of the increased division at the surface could be nutrient based. Indeed, if some essential nutrients penetrate only over a finite distance because of their consumption, this will define a region of increased division rate as observed experimentally. Nevertheless, it seems less probable that the reduction of proliferation with pressure is linked to a stress-dependent depletion of nutrients. To rule out this hypothesis we use a fluorescently labeled growth factor (Alexa 555-EGF) in physiological concentration and verify that its transport is not affected by stress. Spheroids are incubated with A555-EGF during 2 days with and without pressure (0 or 1 kPa). We show in figure 7 that after this incubation EGF is present in all of the spheroid and therefore that stress does not significantly reduce the penetration of this growth factor. Even if we cannot exclude an effect of stress on the permeation of a different growth factor, this result supports the idea that a direct mechanical effect may be the cause of proliferation reduction in the presence of stress.

## 4. Conclusion

This work provides three main results: a constant mechanical stress reversibly reduces growth, the concept of the homeostatic pressure can be extended to take into account surface effects and the increased surface division can be explained mechanically.

Under the action of a constant external isotropic stress, cell aggregates of the colon carcinoma cell line CT26 duplicate in the bulk much slower than in the absence of stress. This effect is reversible. More accurately, for a 10 kPa stress the duplication rate in the bulk drops by a factor as large as 300, while the apoptosis rate does not change significantly.

Then, this work is the first attempt to test the concept of homeostatic pressure [14]. We show that a significant extension to that concept is needed, particularly in view of surface effects. We find that the bulk homeostatic pressure of the studied cell line is too small to explain the growth dynamics. Instead, growth is dominated by surface division. Our spheroids show a negative growth in the bulk for all applied stresses. Thus the bulk homeostatic stress has to be smaller than the stress inside the spheroid: the two main contributions to the pressure inside the spheroid are Laplace pressure due to surface tension and compressional flow. We estimate that the homeostatic stress is smaller than a few Pascals or is possibly negative. That is to say, in order for the division rate to balance the apoptotic rate *in bulk*, the tissue needs to be under tensile stress. In practice, the bulk of the tissue is maintained by an influx of cells from the surface. Indeed, the simulated tissue used to match the experiments has a negative homeostatic pressure, which effect may be studied in a separate work. Still this phenomenon would have be investigated in the context of different cell lines.

Furthermore, we observe a 'skin' effect: in a thin region near the aggregates surface the duplication rate is much larger than in the bulk, typically by a factor of 2 at zero stress. Thus, in the framework of Basan *et al*, we propose that there are two distinct homeostatic stresses: one for the bulk and one for the 'skin'. The duplication rate increment depends much less on stress than the bulk rate. A possible explanation is that nutrients or growth factors penetrate only over a finite length into the aggregate, thereby defining the skin region. However, our simulations point to another contribution: in the absence of any biochemical signaling, the region of the 'numerical aggregate' close to the surface duplicates much faster than in the bulk. This is a purely mechanical effect which we can understand from purely mechanical considerations. To grow, a cell must deform its environment. The deformation is facilitated if the cell is close to the surface, and this implies that proliferation is favored at the surface. Our simulations show that this effect is not small and is completely compatible with our experimental observations. One is naturally led to wonder if such an effect may exist *in vivo*. The answer is likely to be positive but hard to pinpoint, being always mixed with biochemical signalization.

Previous experiments have measured the stress developed by a growing spheroid in an elastic medium [9–11]. Although reported measurements are based on a different ensemble the magnitude of the stress needed to stop the spheroid growth is compatible with our results. Finally, in a recent study, a localized increase of mitochondrial apoptosis and a strong reduction of proliferation in the presence of stress were reported [11]. We find only a small increase in apoptosis as a function of stress. This difference may be due to the use of different cell lines, or different experimental protocols. We work at constant applied stress, whereas in [11], the stress increases with aggregate size. New developments may allow us to measure simultaneously in a living tissue the division and the apoptosis rates and to get a more accurate value and spatial dependence. This might allow for an improvement in our simulations and a more detailed comparison. Our results favor the idea that mechanical effects can have strong implications in cancer proliferation. It is natural to question the relevance of spheroids as model systems. Our results show that the surface plays a central role in their growth process. Surface conditions are clearly very different in most *in vivo* situations. One might be tempted then to simply dismiss this type of *in vitro* experiments. This should not be the case for two reasons: firstly, one does learn how to apprehend quantitatively the long-term dynamics of cell populations; secondly, some *in vivo* situations may turn out to be very close to those observed here, for instance growth after surgery.

**IOP** Institute of Physics  Φ DEUTSCHE PHYSIKALISCHE GESELLSCHAFT

## Acknowledgments

## References

[1] Farge E 2011 Mechanotransduction in development *Curr. Top. Dev. Biol.* **95** 243–65

[2] Butcher D T, Alliston T and Weaver V M 2009 A tense situation: forcing tumour progression *Nature Rev. Cancer* **9** 108–22

[3] Chauvière A, Preziosi L and Verdier C 2009 *Cell Mechanics: From Single Scale-Based Models to Multiscale Modeling* vol 32 (Boca Raton, FL: CRC Press)

[4] Eaves G 1973 The invasive growth of malignant tumours as a purely mechanical process *J. Pathology* **109** 233–7

[5] Young J S 1959 The invasive growth of malignant tumours: an experimental interpretation based on elastic-jelly models *J. Pathol. Bacteriol.* **77** 321–39

[6] Whitehead J, Vignjevic D, Fütterer C, Beaurepaire E, Robine S and Farge E 2008 Mechanical factors activate beta-catenin-dependent oncogene expression in APC mouse colon *HFSP J.* **2** 286–94

[7] Mueller M M and Fusenig N E 2004 Friends or foesbipolar effects of the tumour stroma in cancer *Nature Rev. Cancer* **4** 839–49

[8] Orimo A and Weinberg R A 2006 Stromal fibroblasts in cancer: a novel tumor-promoting cell type *Cell Cycle* **5** 1597–601

[9] Helmlinger G, Netti P A, Lichtenbeld H C, Melder R J and Jain R K 1997 Solid stress inhibits the growth of multicellular tumor spheroids *Nature Biotechnol.* **15** 778–83

[10] Fritsch A, Hockel M, Kiessling T, Nnetu K D, Wetzel F, Zink M and Kas J A 2010 Are biomechanical changes necessary for tumour progression? *Nature Phys.* **6** 730–2

[11] Cheng G, Tse J, Jain R K and Munn L L 2009 Micro-environmental mechanical stress controls tumor spheroid size and morphology by suppressing proliferation and inducing apoptosis in cancer cells *PloS One* **4** e4632

[12] Demou Z N 2010 Gene expression profiles in 3D tumor analogs indicate compressive strain differentially enhances metastatic potential *Ann. Biomed. Eng.* **38** 3509–20

[13] Roose T, Netti P A, Munn L L, Boucher Y and Jain R K 2003 Solid stress generated by spheroid growth estimated using a linear proelasticity model *Microvascular Res.* **66** 204–12

[14] Basan M, Thomas Risler, Joanny J-F, Sastre-Garau X and Prost J 2009 Homeostatic competition drives tumor growth and metastasis nucleation *HFSP J.* **3** 265–72

[15] Byrne H M 2010 Dissecting cancer through mathematics: from the cell to the animal model *Nature Rev. Cancer* **10** 221–30

[16] Galle J, Hoffmann M and Aust G 2009 From single cells to tissue architecture—a bottom-up approach to modelling the spatio-temporal organisation of complex multi-cellular system *Math. Biol.* **58** 261–83

[17] Galle J, Loeffler M and Drasdo D 2005 Modeling the effect of deregulated proliferation and apoptosis on the growth dynamics of epithelial cell populations *in vitro Biophys. J.* **88** 62–75

[18] Drasdo D, Hoehme S and Block M 2007 On the role of physics in the growth and pattern formation of multi-cellular systems: what can we learn from individual-cell based models? *J. Stat. Phys.* **128** 287–345

[19] Chaplain M A, Graziano L and Preziosi L 2006 Mathematical modelling of the loss of tissue compression responsiveness and its role in solid tumour development *Math. Med. Biol.* **23** 197–229

[20] Byrne H and Drasdo D 2009 Individual-based and continuum models of growing cell populations: a comparison *J. Math. Biol.* **58** 657–87

[21] Basan M, Prost J, Joanny J-F and Elgeti J 2011 Dissipative particle dynamics simulations for biological tissues: rheology and competition *Phys. Biol.* **8** 026014

**IOP** Institute of Physics  **Φ** DEUTSCHE PHYSIKALISCHE GESELLSCHAFT

[22] Drasdo D and Höhme S 2005 A single-cell-based model of tumor growth *in vitro*: monolayers and spheroids *Phys. Biol.* **2** 133–47

[23] Schaller G and Meyer-Hermann M 2005 Multicellular tumor spheroid in an off-lattice Voronoi–Delaunay cell model *Phys. Rev.* E **71** 1–16

[24] Ranft J, Basan M, Elgeti J, Joanny J F, Prost J and Jülicher F 2010 Fluidization of tissues by cell division and apoptosis *Proc. Natl. Acad. Sci. USA* **107** 20863–8

[25] Montel F *et al* 2011 Stress clamp experiments on multicellular tumor spheroids *Phys. Rev. Lett.* **107** 188102

[26] Hirschhaeuser F, Menne H, Dittfeld C, West J, Mueller-Klieser W and Kunz-Schughart L A 2010 Multicellular tumor spheroids: an underestimated tool is catching up again *J. Biotechnol.* **148** 3–15

[27] Bonnet-Gonnet C, Belloni L and Cabane B 1994 Osmotic pressure of latex dispersions *Langmuir* **10** 4012–21

[28] Bouchoux A , Cayemitte P-E, Jardin J , Gésan-Guiziou G and Cabane B 2009 Casein micelle dispersions under osmotic stress *Biophys. J.* **96** 693–706

[29] Montel F, Fontaine E, St-Jean P, Castelnovo M and Faivre-Moskalenko C 2007 Atomic force microscopy imaging of SWI/SNF action: mapping the nucleosome remodeling and sliding *Biophys. J.* **93** 566–78

[30] Freyer J P and Sutherland R M 1986 Regulation of growth saturation and development of necrosis in EMT6/Ro multicellular spheroids by the glucose and oxygen supply *Cancer Res.* **46** 3504

[31] Casciari J J, Sotirchos S V and Sutherland R M 1992 Mathematical modelling of microenvironment and growth in EMT6/Ro multicellular tumour spheroids *Cell Proliferation* **25** 1–22

[32] Cowan K J 2003 Mitogen-activated protein kinases: new signaling pathways functioning in cellular responses to environmental stress *J. Exp. Biol.* **206** 1107–15

[33] Racz B, Reglodi D, Fodor B, Gasz B, Lubics A, Gallyas F, Roth E and Borsiczky B 2007 Hyperosmotic stress-induced apoptotic signaling pathways in chondrocytes *Bone* **40** 1536–43

[34] Nielsen M-B, Christensen S T and Hoffmann E K 2008 Effects of osmotic stress on the activity of MAPKs and PDGFR-beta-mediated signal transduction in NIH-3T3 fibroblasts *Am. J. Physiol.* **294** C1046–55

[35] Xie Y, Zhong W, Wang Y, Trostinskaia A, Wang F, Puscheck E E and Rappolee D A 2007 Using hyperosmolar stress to measure biologic and stress-activated protein kinase responses in preimplantation embryos *Mol. Hum. Reprod.* **13** 473–81

[36] Mueller-Klieser W 1997 Three-dimensional cell cultures: from molecular mechanisms to clinical applications *Am. J. Physiol.* **273** C1109–23

[37] Mollica D and Ambrosi F 2004 The role of stress in the growth of multicell spheroid *Math. Biol.* **48** 477–99

[38] Radszuweit M, Block M, Hengstler J G, Schöll E and Drasdo D 2009 Comparing the growth kinetics of cell populations in two and three dimensions *Phys. Rev.* E **79** 051907

[39] Bertalanffy V L 1957 Quantitative laws in metabolism and growth *Q. Rev. Biol.* **32** 217–31

[40] Dorie M J, Kallman R F, Rapacchietta D F, Van Antwerp D and Huang Y R 1982 Migration and internalization of cells and polystyrene microsphere in tumor cell spheroids *Exp. Cell Res.* **141** 201–9